Lawrence Berkeley National Laboratory

Title

Beta-Delayed Proton Decay of {sup 25}Si

Permalink

Journal

Authors

Robertson, J.D.
Moltz, Dennis M.
Lang, T.F.
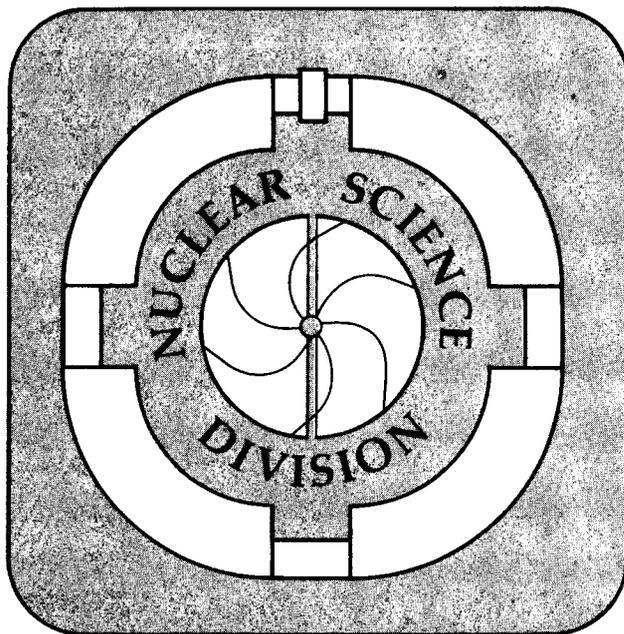et al.

Publication Date

Lawrence Berkeley Laboratory
UNIVERSITY OF CALIFORNIA

Beta-Delayed Proton Decay of ^{25}Si

J.D. Robertson, D.M. Moltz, T.F. Lang, J.E. Reiff,
J. Cerny, and B.H. Wildenthal

September 1992

DISCLAIMER

DISCLAIMER

Beta-Delayed Proton Decay of ^{25}Si

J.D. Robertson, D.M. Moltz, T.F. Lang, J.E. Reiff, Joseph Cerny

Department of Chemistry
University of California

and

Nuclear Science Division
Lawrence Berkeley Laboratory
University of California
Berkeley, CA 94720

and

B.H. Wildenthal

School of Natural Sciences and Mathematics
University of Texas at Dallas
Richardson, TX 75083-0688

September 1992

Beta-Delayed Proton Decay of ^{25}Si

J.D. Robertson,[*] D.M. Moltz, T.F. Lang,[†] J.E. Reiff,[‡] and Joseph Cerny
Department of Chemistry and Nuclear Science Division
University of California
Berkeley, CA 94720

and

B.H. Wildenthal

School of Natural Sciences and Mathematics
University of Texas at Dallas
Richardson, TX 75083-0688

We have measured the beta-delayed proton spectrum arising from ^{25}Si produced in the ^{24}Mg(^{3}He,2n) reaction. Utilization of a new low-energy proton detector has permitted the observation of protons from 250–6000 keV. Most proton groups have been placed into a decay scheme by using penetrability calculations and transitions from the mirror beta decay, ^{25}Na → ^{25}Mg. This placement permits the construction of the Gamow-Teller strength function which we compare to a beta strength function calculated from complete-space s-d shell model wave functions.

I. INTRODUCTION

The experimental study of Gamow-Teller (GT) beta decay is important to a fundamental understanding of nuclear structure. Because the mediator of Gamow-Teller transitions, an operator which flips both spin and isospin, is relatively simple and restrictive in its action, it provides a particularly sensitive test of the wave functions used in nuclear structure calculations. At the most detailed level, when the individual final states in the beta daughter can be experimentally identified, measured strength provides information about the degree of overlap between the initial and final nuclear states. This type of detailed transition-by-transition comparison has been performed by Brown and Wildenthal for the nuclei in the $2s1d$ shell [1]. At a more comprehensive level, when beta Q values provide access to a significant range of excitation energies in the daughter nucleus, then the distribution of the matrix element values versus energy, the "GT strength function", yields information about the global response of the parent wave function to spin-isospin excitation.

We have recently measured the beta-delayed proton decay of the Tz = –3/2 nuclide ^{25}Si in order to compare the observed GT strength function to that predicted by full space $d_{5/2}$-$s_{1/2}$-$d_{3/2}$ shell model calculations. Typical allowed beta decays occur with small Q values such that only the lowest few levels in the daughter system are populated. The dominant spin-flip nature of the GT process implies, however, that most of the GT transition strength will be found at an excitation energy characteristic of the spin-orbit splitting, about 7 to 10 MeV in the sd shell. Consequently, although the investigations of the beta decays with low Q values frequently permit the detailed comparison mentioned above, they only sample a small fraction of the total allowed GT strength. On the other hand, the beta decay of ^{25}Si, with its Q value of 12.7 MeV, offers the chance to observe the GT decay to a significant fraction of the levels in the daughter system and determine whether the energy distribution of the dominant portion of the strength agrees with prediction. Moreover, although phase space factors favor beta decay to lower-lying levels in the daughter ^{25}Al, the full basis shell model calculations predict that a major portion of the GT decay, over 25%, will occur to states in ^{25}Al that lie above the proton separation energy in the

2

daughter. By measuring the delayed protons it has been possible to extract accurate β-decay branching ratios to states up to 8.2 MeV in ^{25}Al.

Silicon-25 was one of the four isotopes which were first reported to decay by beta-delayed proton emission in 1963 [2]. This decay branch of ^{25}Si was subsequently investigated in several works [3–7] with the most extensive study to date being that of Reeder *et al.* in 1966 [7]. In this work, the β^+-p spectrum was measured from 0.7 to 6.0 MeV with a resolution of 85 keV full-width-half-maximum (above 1.7 MeV) and 18 proton groups were assigned to the decay of ^{25}Si. With the development of a new, low-energy proton-detector telescope, we have been able to measure the proton spectrum for ^{25}Si from 0.25 to 6.0 MeV with an average resolution of 51 keV FWHM over the entire energy range. As a result of the improved resolution and lower energy cutoff, we were able to identify 14 new proton groups in addition to those assigned to ^{25}Si decay previously [7].

II. EXPERIMENTAL PROCEDURE

Silicon-25 was produced via the ^{24}Mg(^{3}He,2n)^{25}Si reaction by bombarding a 1.6-mg/cm^2-thick natural magnesium target with a 40-MeV ^{3}He^{2+} beam from the Lawrence Berkeley Laboratory 88-Inch Cyclotron. The reaction products were collected and transported to a low-background counting station using a He-jet transport system which is described in detail elsewhere [8]. Briefly, the magnesium target was located in a chamber pressurized to 1.3 atm with helium. Reaction products which recoiled out of the target and thermalized in the helium gas were transported on KCl aerosols suspended in the gas through a 40 cm long, 1.0 mm i.d. capillary to the counting chamber, which was maintained at a pressure of 10^{-3} atm. The mean transport delay time of this system was on the order of 30 ms. In order to minimize the loss of the short-lived ^{25}Si, the transported activities were collected on a rotating wheel directly in front of the detector telescope as illustrated in Figure 1. The catcher wheel, which removes long-lived β^+ activities from in front of the detector telescope, was rotated at a rate of one revolution per 39 seconds.

The detector telescope used in the experiment was a new. low-energy particle-identification telescope which we have developed primarily to measure low-energy protons in a high radiation environment [9]. As can be seen from Fig. 1, it consists of a gas ΔE detector and a 300 μm Si E detector. The active volume of the gas ΔE is defined by two wire grids 2.5 mm on either side of a 70 $\mu g/cm^2$-thick nickel foil The wire grids are grounded and the nickel electrode is maintained at a potential of 540 volts. This high electric field (~2000 V/cm) places the gas detector just below the avalanche region and provides the gas amplification necessary for particle identification. As can be seen from the two-dimensional ΔE-E spectrum shown in Figure 2, the proton band from the telescope is clearly separated from the β^+/e^- band and alpha band. Isobutane, Freon-14 (CF$_4$), propane, and an argon-methane mixture were tested as gases for the ΔE counter and it was found that Freon-14 gave the best gas amplification for protons with a shaping time comparable to that used for the silicon counter.

In this new proton telescope, the signals for the ΔE counter are used for particle identification but the final energy signal is taken solely from the silicon E counter as the protons lose so little energy in the gas ΔE counter. Most of the energy loss is in the entrance window and Ni electrode thereby making the 16 keV lost by a 300-keV proton and the 8 keV lost by a 4 MeV proton in the gas of the ΔE counter insignificant. All of these differential energy losses are built into the energy calibration. This telescope design has been used to successfully measure protons whose energies range from 250 keV to 5.5 MeV in a β^+ background of 10^5 cps. The new telescope has the advantage over the solid state particle identification telescopes used in our previous proton measurements, *e.g.*, reference [10,11], in that it allows us to measure protons with energies less than 700 keV on an event-by-event basis.

The overall performance of the system and calibration of the proton telescope was established by measuring the β^+-p decay of ^{29}S [10]. The proton spectrum shown in Fig. 3 arose from the bombardment of a 2-mg/cm^2-thick natural silicon target with a 5 μA 40 MeV ^{3}He^{2+} beam. This spectrum was generated by simply gating on the proton band in the two-dimensional ΔE-E spectrum. Given that the known, lowest energy proton group for ^{29}S decay is at 739 keV, the

4

efficiency response of the detector telescope for protons below this energy was established by separate proton scattering measurements. These Rutherford scattering experiments were performed at the Tandem Van de Graaff accelerator at the Lawrence Livermore National Laboratory. In these calibrations, proton beams of known relative intensities whose energies ranged from 350 keV to 2 MeV were produced by scattering protons from a 20-μg/cm^2-thick graphite foil From these scattering measurements and the ^{29}S β^+-p measurements, we were able to determine that the efficiency of the proton-telescope remains constant as the proton energy varies from 350 keV to 5.5 MeV.

III. EXPERIMENTAL RESULTS

The proton spectrum obtained from the bombardment of a 1.7-mg/cm^2-thick natural magnesium-target with a 2.5 μA 40 meV ^{3}He^{2+} beam is shown in Fig. 4. Again, this spectrum was generated by simply gating on the proton band in the two-dimensional ΔE-E spectrum (see Fig. 2). A beam energy of 40 MeV was chosen in order to maximize the production rate of ^{25}Si. According to the fusion-evaporation code ALICE [12], the cross section for the ^{24}Mg(^{3}He,2n)^{25}Si reaction peaks at or near this energy. At 40 MeV, the beam is energetic enough to also produce the β^+-p emitters ^{21}Mg [13] and ^{24}Si [14] via the ^{24}Mg(^{3}He,α2n) and ^{24}Mg(^{3}He,3n) reactions, respectively. However, no proton peaks attributed to the decay of either of these species were observed in the spectrum shown in Fig. 4. The only other β^+-p emitter that could be produced at this beam energy is ^{17}Ne [15] via the (^{3}He,2n) reaction with any oxygen contamination in the target or carrier gas. Because neon is not transported in the helium-jet, proton peaks associated with the decay of ^{17}Ne could not have been observed even if it had been produced. Because no β^+-p "contaminants" were identified in the accumulated spectrum, all of the peaks in Fig. 4 were assigned to the decay of ^{25}Si.

The energies and relative intensities of the proton groups assigned to ^{25}Si decay are listed in Table I. In addition to the ^{29}S data, the intense peaks at 0.906, 1.848, 2.219, and 4.088 MeV were also used in the energy calibration. The energies of these transitions are known from the well determined states in ^{25}Al [16]. A total of 14 new proton groups has been assigned to the decay of

[25]Si but we did not observe the groups at 0.79 and 5.66 MeV reported previously [7]. Clearly, the peak at 0.79 MeV should have been readily observed if it did belong to [25]Si β^+-p decay with a relative intensity of 14%.

In addition to the new proton groups, the major difference between this work and that of Reeder et al. [7] is the reported relative intensities for the proton groups. As can be seen from Table I, our intensity values, normalized to the 4.09 MeV group, are in all cases less than the values reported in reference [7]. One possible source for this discrepancy could be an erroneously large value for the strength of the 4.09 MeV peak in the spectrum shown in Fig. 4. Yet, if this were the case, then the ratios of our relative intensities to those reported in reference [7] should be fairly constant. Such a comparison for those groups whose relative intensities are greater than 10% yields ratios that range from 1.0 to 3.6 (with no correlation with energy). Moreover, one would expect that a large value for the 4.09-MeV peak would arise from some β^+-p "contaminant" in our spectrum. Yet, the only known β^+-p emitter that yields a proton group that could not be readily resolved from the 4.09-MeV peak is [20]Mg. The difference in energy between its main proton group at 4.16 MeV and the 4.09-MeV peak would be less than twice the FWHM resolution of 51 keV. However, [20]Mg cannot be produced at this energy as the minimum laboratory energy required for the [24]Mg([3]He,α3n) reaction is 49 MeV. We therefore conclude that the differences in the relative intensities reported in Table I are most likely due to the poorer detector resolution in the previous work. That is, the intensity values reported for individual peaks in reference [7] most likely include contributions from several groups.

The proton transition assignments and deduced [25]Al level excitation energies are given in Table II. The individual assignments are based upon energy sum relationships with the known levels in the beta and proton daughter nuclei [16]. In the majority of cases, each assignment is uniquely determined given the uncertainty in the observed proton energies and the energies of the levels in [25]Al. Of the eight proton groups whose assignments are not uniquely determined, seven have been placed in the proposed level scheme shown in Fig. 5. Because the proton peak at

2.28 MeV cannot arise from the decay of any of the known levels in ^{25}Al [16], it was not placed in the decay scheme.

The 0.37-MeV proton peak is the lowest energy proton group seen thus far in β^+-p decay studies. Considering only energy sum relationships, this peak could arise from the decay of ^{25}Al levels at 2.67, 4.03, 6.77, and 7.90 MeV. Yet, since the 0.37-MeV peak is the second most intense peak in the proton spectrum, we conclude from the following that it must originate from a level in ^{25}Al that can only decay to the g.s. in ^{24}Mg and have assigned it to the decay of the 2.67 MeV state. On the basis of penetrability calculations *alone*, the 5/2$^+$ 4.03 MeV level is estimated to be 200 times more likely to decay to the g.s. of ^{24}Mg ($\Delta l = 2$) than to decay to the first 2$^+$ state ($\Delta l = 0$). Because the g.s. proton branch was not observed, we conclude that the 0.37-MeV proton peak does not arise from the decay of this level to the first 2$^+$ state. The same argument can be used to rule out assigning this transition to the decay of the 6.77- and 7.90-MeV levels in ^{25}Al.

The β-decay transition rates to the proton unbound levels are directly related to the proton intensities as γ decay does not complete favorably with proton decay for states which are unbound by more than ~500 keV [10]. Moreover, because the absolute branching ratio to the analog state can be calculated nearly model independently, absolute branching ratios can be obtained by comparing the observed proton intensity for each level with the proton intensity observed for the decay of the analog state. The probability of super-allowed beta decay to the isobaric analog state in the daughter is a function of the Fermi and Gamow-Teller matrix elements. Neglecting isospin mixing, the Fermi matrix element connecting members of the same isobaric multiplet is given by

$$<\tau>^2 = T(T + 1) - T_{zi}T_{zf} \tag{1}$$

where T_{zi} and T_{zf} are the initial and final z-component isospin projections ($= (N - Z)/2$). In the case of ^{25}Si, $<\tau>^2 = 3$. Although the Gamow-Teller matrix element $<\sigma\tau>^2$ depends on the inherent details of the wave functions and its evaluation is, therefore, model dependent, it makes only a small contribution. Recent shell model calculations of Wildenthal [17] predict a quenched value of $<\sigma\tau>^2$ of 0.11, while an earlier estimate using the Nilsson formalism [4] gave $<\sigma\tau>^2$ of 0.16.

Fortunately, because of the magnitude of the Fermi contribution in superallowed β decay, uncertainties in $< \sigma\tau >^2$ of this magnitude change the ft value by only 3% and the log ft by < 0.01. As a result, the superallowed transition rate can be calculated nearly model independently. A log ft of 3.28 predicted from the full basis shell model calculations has been used to estimate the absolute branching ratio to the $T = 3/2$, 7.901 MeV state in ^{25}Al. The corresponding branching ratios to the remaining unbound levels were determined through a comparison of the proton intensities (Table I). Branching ratios to the proton bound levels were calculated by assuming that the log ft to these levels is identical to that in the mirror decay of ^{25}Na → ^{25}Mg [18] when corrected for the appropriate ft^+/ft^- ratio. If we utilize the measured value of 1.207 [18] rather than the averaged value of 1.085 taken as an extrapolation of other measurements in this mass region [18], then the branching ratios given in Table III need no renormalization.

The one level above the proton separation energy in ^{25}Al for which the gamma decay probability is not negligible is the 2.674 MeV level. The Γ_γ/Γ_p ratio of this state has been measured by proton scattering to be 0.12. This ratio, coupled with the measured proton decay branch, yields a beta branch to this level of 8.2 ± 1.5%. This value is in excellent agreement with a value of 8.3 ± 1.5% predicted from comparison with the mirror beta decay of ^{25}Na. A value of 8.2% was used in all calculations.

As has already been referenced, there are many early studies of ^{25}Si beta-delayed proton decay (e.g., ref. [7]). There also exists, however, an unpublished study [19] of ^{25}Si delayed proton decay. In this work, ^{25}Si was collected via the helium-jet technique on a catcher wheel rotated by a fast stepping motor. Unlike the present experiment in which the detector viewed the collection spot, the previous experiment [19] only detected protons rotated in front of a detector telescope. The half-life determined in this experiment was 222.6 ± 5.9 ms. Combining this result with two previous results [3,7] which all agree, yields a weighted average of 220.7 ± 2.9 ms. This half-life was used to calculate the partial half-lives and log ft values for each transition given in the decay scheme shown in Fig. 5. The log ft values are also listed in Table III. The phase space factors

were calculated using previously outlined methods [20–22] as discussed by Brown and Wildenthal [1].

IV. DISCUSSION AND CONCLUSION

For each level in ^{25}Al populated in ^{25}Si beta decay, we have deduced the corresponding Gamow-Teller matrix elements. These matrix elements are given in Table III. Plotting the sum of these Gamow-Teller matrix elements per unit of daughter excitation energy is the most common representation of the Gamow-Teller strength function. The strength function derived from ^{25}Si beta-delayed proton decay is depicted in the top half (experimental) of Fig. 6. The bottom part of Fig. 6 represents an equivalent binning of the quenched Gamow-Teller strength derived from matrix elements calculated utilizing complete sd shell model wave functions [17].

These wave functions are obtained from a physically realizable comprehensive calculation of all sd-shell states which was carried out in the complete space of $0d_{5/2} - 1s_{1/2} - 0d_{3/2}$ configurations with a single, smoothly mass dependent Hamiltonian. The mass dependence consisted of scaling all two-body matrix elements by the factor $(A/18)^{-0.3}$. The eigenvalues obtained from diagonalizing this " universal sd " (USD) or " Wildenthal " Hamiltonian in the complete sd-shell space agree quite well with observed energies of analogous experimental levels for all nuclei in the shell. In addition, the eigenfunctions yield matrix elements for observables such as single-nucleon spectroscopic factors and E2 and M1 moments and transition rates which agree well with corresponding experimental values.

Comparison of Gamow-Teller strengths calculated from these wave functions with beta decay experimental results from low Q-value transitions has shown that the relative strenths predicted from the wave functions agree with the relative strenths measured in experiment, but that the absolute theoretical strengths are larger than those observed by a factor which is reasonably constant over the entire shell. The " quenching factor ", or " renormalization ", which is needed in order to bring the predicted absolute strengths into agreement with experiment is 0.60. This empirical factor is quite consistent with theoretical estimates of the effects of many $\hbar\omega$

core polarization and of mesonic-exchange-current effects. It is these quenched USD predictions which are plotted in Fig. 6.

The general agreement between the measured and calculated beta strength functions is excellent. In fact the summed strength is predicted exactly. The minor differences in the plots are due principally to the binning used to depict the data. The small differences above 9 MeV are probably due to experimental non-observation. Populated states at these high excitation energies probably emit protons to higher-lying states, which are thus masked by other transitions. (Although the beta strength may be appreciable, the absolute branching ratios are quite small).

We have observed the beta-delayed proton decay of ^{25}Si. These results have been utilized to construct a decay scheme and beta strength function which has been accurately reproduced with a complete sd shell model calculation which assumes a previously determined quenching factor for sd-shell beta decay. This experiment was made possible by the development of a low-energy proton detector which could identify protons with kinetic energies as low as 250 keV. Given the major branch corresponding to the 367 keV group, this detector was essential. Finally, during the last stages of preparation of this document, another manuscript on the decay of ^{25}Si was discovered as part of the proceedings of a recent conference [25]. Since the details of this work are incomplete, a direct comparison cannot be made.

REFERENCES

*Present Address: Department of Chemistry, University of Kentucky, Lexington, KY 40506.

†Present Address: UCSF Physics Research Laboratory, 389 Oyster Point Blvd., South San Francisco, CA 94080.

‡Present Address: Department of Medical Physics, Memorial Sloan Kettering Cancer Center, 1275 York Ave., New York, NY 10021.

[1] B.A. Brown and B.H. Wildenthal, ADNDT **33**, 348 (1985).

[2] R. Barton, R. McPherson, R.E. Bell, W.R. Frisken, W.T. Link and R.B. Moore, Can. J. Phys. **41**, 2007 (1963).

[3] R. McPherson and J.C. Hardy, Can. J. Phys. **43**, 1 (1965).

[4] J.C. Hardy and B. Margolis, Phys. Lett. **15**, 276 (1965).

[5] J.C. Hardy and R.E. Bell, Can. J. Phys. **43**, 1671 (1965).

[6] R.S. Bender, I.R. Williams and K.S. Toth, Nucl. Instr. and Meths. **40**, 241 (1966).

[7] P.L. Reeder, A.M. Poskanzer, R.A. Esterlund and R. McPherson, Phys. Rev. **147**, 781 (1966).

[8] M.D. Cable, J. Honkanen, E.C. Schloemer, M. Ahmed, J.E. Reiff, Z.Y. Zhou, and J. Cerny, Phys. Rev. C **30**, 1276 (1984).

[9] J.E. Reiff, M.A.C. Hotchkis, D.M. Moltz, T.F. Lang, J.D. Robertson, and Joseph Cerny, Nucl. Instrum. Meth. **A276**, 228 (1989).

[10] D.J. Viera, R.A. Gough and J. Cerny, Phys. Rev. C **19**, 177 (1979).

[11] J. Äystö, X. J. Xu, D. M. Moltz, J. E. Reiff, Joseph Cerny, and B. H. Wildenthal, Phys. Rev. C **32**, 1700 (1985).

[12] M. Blann and J. Birplinghoff, LLNL Report No. UCID-19614, 1982 unpublished.

[13] R.G. Sextro, R.A. Gough, and Joseph Cerny, Phys. Rev. C **8**, 258 (1972).

[14] J. Äystö, D.M. Moltz, M.D. Cable, R.D. von Dincklage, R.F. Parry, I.M. Wouters, and J. Cerny, Phys. Lett. **82B**, 43 (1979).

[15] J.C. Hardy, J.E. Esterl, R. G. Sextro, and Joseph Cerny, Phys. Rev. C **3**, 700 (1971).

[16] P.M. Endt , Nucl. Phys. **A521**, 1 (1990).

[17] B. H. Wildenthal, Progress in Particle and Nuclear Physics, Vol. II, ed. by D. H. Wilkinson (Pergamon Press, Oxford, 1984), p. 5.

[18] D.E. Alburger and D.H. Wilkinson, Phys. Rev. C 3, 1957 (1971).

[19] R.G. Sextro, Ph.D. Thesis, Lawrence Berkeley Laboratory Report LBL-2360 (1973) unpublished.

[20] D.H. Wilkinson, Nucl. Phys. A209, 470 (1973).

[21] D.H. Wilkinson and B.E. F. Macefield, Nucl. Phys. A232, 58 (1974).

[22] D.H. Wilkinson, Nucl. Phys. A377, 474 (1982).

[23] A.H. Wapstra and G. Audi, Nucl. Phys. A432, 1 (1985).

[24] Z.Y. Zhou, E.C. Schloemer, M.D. Cable, M. Ahmed, J.E. Reiff and J. Cerny, Phys. Rev. C 31, 1941 (1985).

[25] S. Hatori, H. Miyatake, T. Shimoda, N. Takahashi, Y. Fujita, and S. Morinobu, to be published in the Proceedings of 6th International Conference on Nuclei far from Stability and 9th International Conference on Atomic Masses and Fundamental Constants, 19-24 July, 1992, Bernkastel-Kues, Germany.

TABLE I. The proton groups assigned to the β^+ delayed proton decay of ^{25}Si. Peak numbers refer to Fig. 4.

Peak No.	Present work		Previous Work[a]	
	Lab proton energy (MeV)	Relative intensity (%)[d]	Lab proton energy (MeV)	Relative intensity (%)
1	0.367 ± 20	73.7 ± 0.3		
2	0.528 ± 25	2.5 ± 0.1		
			0.79	14
3	0.9057[b]	17.0 ± 0.1	0.93	23
4	0.998 ± 20	1.53 ± 0.03		
5	1.221 ± 20	2.26 ± 0.07		
6	1.340 ± 20	2.89 ± 0.05		
7	1.441 ± 20	2.90 ± 0.05		
8	1.528 ± 20	1.46 ± 0.03		
9	1.617 ± 20	0.93 ± 0.06		
10	1.732 ± 15	6.73 ± 0.06	1.73	11
11	1.8482[b]	27.4 ± 0.1	1.87	40
12	2.078 ± 10	17.2 ± 0.1	2.09	24
13	2.2189[b]	14.1 ± 0.1	2.22	25
14	2.278 ± 20[c]	2.02 ± 0.03		
15	2.355 ± 25	0.40 ± 0.02		
16	2.386 ± 25	0.96 ± 0.02		
17	2.504 ± 25	0.39 ± 0.05		
18	2.900 ± 15	3.74 ± 0.09	2.90	10
19	3.108 ± 15	4.15 ± 0.05	3.13	15
20	3.208 ± 15	6.57 ± 0.06		
21	3.328 ± 10	34.5 ± 0.1	3.33	39
22	3.453 ± 10	10.86 ± 0.08	3.48	11
23	3.709 ± 20	1.15 ± 0.07	3.70	8
24	4.0881[b]	100.0 ± 0.20	4.08	100
25	4.131 ± 20	3.32 ± 0.07		
26	4.374 ± 20	1.28 ± 0.05	4.35	7
27	4.441 ± 25	0.25 ± 0.01		
28	4.659 ± 15	7.29 ± 0.07	4.63	17
29	4.792 ± 15	2.30 ± 0.04	4.75	2
30	5.178 ± 20	1.98 ± 0.05	5.10	6
31	5.327 ± 15	3.19 ± 0.06		
32	5.404 ± 10	16.9 ± 0.2	5.35	20
			5.66	2

[a]Reference [7].
[b]These proton energies were used, in part, to determine the energy calibration.
[c]This proton group has not been assigned to a transition in ^{25}Si β-p decay.
[d]For absolute intensity per 100 decays multiply by 0.099.

TABLE II. Observed proton energies from the decay of unbound levels in ^{25}Al to various final states in ^{24}Mg and a comparison of deduced level energies in ^{24}Mg with previous results.

| Center of mass proton energies from the decay of ^{25}Al to the following states in ^{24}Mg | | | | Deduced excitation energies in ^{25}Al | | |
g.s. (0+)	1.368 (2+)	4.113 (4+)	4.238 (2+)	Present work[a]	Previous work[b]	$J^\pi;T$ [b]
0.382				2.653±20	2.674±1	3/2+
1.592				3.863±20	3.859±1	5/2+
1.9252[c]	0.550			4.190±25	4.196±3	3/2+
2.3114[c]	0.9434[c]			4.583	4.583±4	5/2+
2.608	1.272			4.899±16	4.906±4	≥5/2+
	2.165			5.805±10	5.809±7	(3/2–7/2)+
	2.453			6.092±25	6.083±7	
3.864	2.486			6.131±16	6.112±7	5/2+
	3.021			6.660±15	6.645±7	(5/2,7/2)+
	3.237			6.877±15	6.881±7	
4.626				6.897±25	6.909±10	3/2+
	3.342			6.982±15	7.022	
4.853	3.466			7.112±8	7.112±10	(3/2-7/2)+
4.992	3.597			7.245±8	7.240±7	(3/2-7/2)+
		1.040		7.434±20	7.417±7	
5.394				7.665±20	7.646	
5.549				7.820±15	7.819±20	
5.630	4.2583[c]	1.501	1.396	7.896±6	7.901±2	5/2+;3/2
	4.303			7.943±20	7.936	
	4.556	1.805	1.685	8.197±10	8.193	(3/2-7/2)+

[a]Calculated using a Q value of 2.2713±1 from Reference [23].
[b]Reference [16].
[c]These proton energies were used, in part, to determine the energy calibration.

TABLE III. Branching ratios and log ft values for the positron decay of ^{25}Si.

^{25}Al Level[a]	Branching ratio (%)[b]	Experimental log ft (sec)	$\langle\sigma\tau\rangle^2$ [e]
0.0	20.8 ± 1.2[c]	5.32 ± 0.03[c]	0.0218
0.945	22.1 ± 1.8[c]	5.12 ± 0.04[c]	0.0346
1.612	17.0±1.4[c]	5.10±0.04[c]	0.0362
1.790	1.7±0.3[c]	6.06±0.04[c]	0.0039
2.674	8.2 ± 1.5	5.19 ± 0.008[c]	0.0248
2.720	<0.4[c]	>6.5[c]	<0.0012
3.859	0.145 ± 0.002	6.66 ± 0.07	0.0008
4.196	2.97 ± 0.02	5.26 ± 0.01	0.0215
4.583	3.10 ± 0.02	5.13 ± 0.01	0.0288
4.906	0.26 ± 0.01	6.11 ± 0.03	0.0031
5.809	1.71 ± 0.01	5.00 ± 0.01	0.0385
6.063	0.04 ± 0.01	6.55 ± 0.03	0.0011
6.123	0.21 ± 0.01	6.01 ± 0.03	0.0061
6.645	0.37 ± 0.01	5.36 ± 0.02	0.0170
6.881	0.41 ± 0.01	5.22 ± 0.02	0.0235
6.909	0.02 ± 0.003	6.43 ± 0.08	0.0015
7.022	0.65 ± 0.01	4.96 ± 0.01	0.0427
7.112	4.15 ± 0.02	4.12 ± 0.01	0.2960
7.240	1.31 ± 0.01	4.56 ± 0.01	0.1060
7.417	0.15 ± 0.01	5.42 ± 0.04	0.0149
7.646	0.20 ± 0.01	5.20 ± 0.04	0.0247
7.819	0.32 ± 0.01	4.90 ± 0.02	0.0485
7.901	12.2	3.28	0.163
7.936	0.33 ± 0.01	4.83 ± 0.02	0.0579
8.193	0.89 ± 0.01	4.26 ± 0.01	0.215
9.065	0.07 ± 0.001[d]	4.80 ± 0.06	0.0617
9.275	0.01 ± 0.002[d]	5.42 ± 0.07	0.0148
9.415	0.01 ± 0.002[d]	5.31 ± 0.07	0.0192

[a]Energies were taken from Reference [16].

[b]The branching ratios and log ft values were calculated for the levels above Sp by assuming complete isospin purity of the T = 3/2 state at 7.901 MeV. The branch to the 1.674 level includes the gamma decay width (see text).
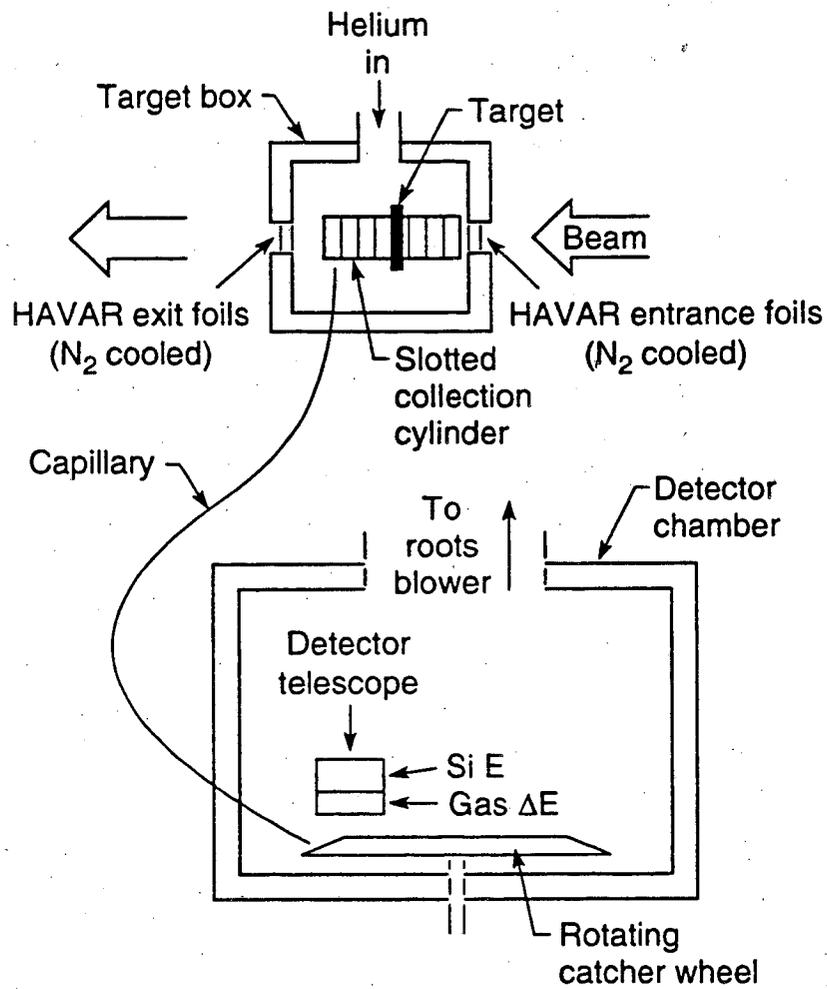
[c]These branching ratios and log ft values were calculated from a comparison to the mirror ^{25}Na decay. Reference [16].

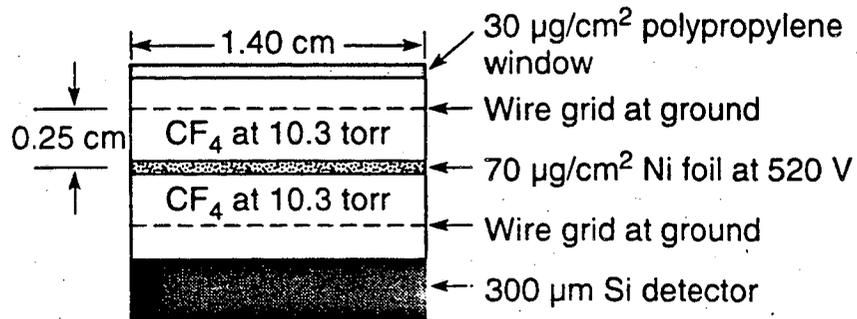[d]These branches were calculated from the proton intensity values reported in Reference [24].
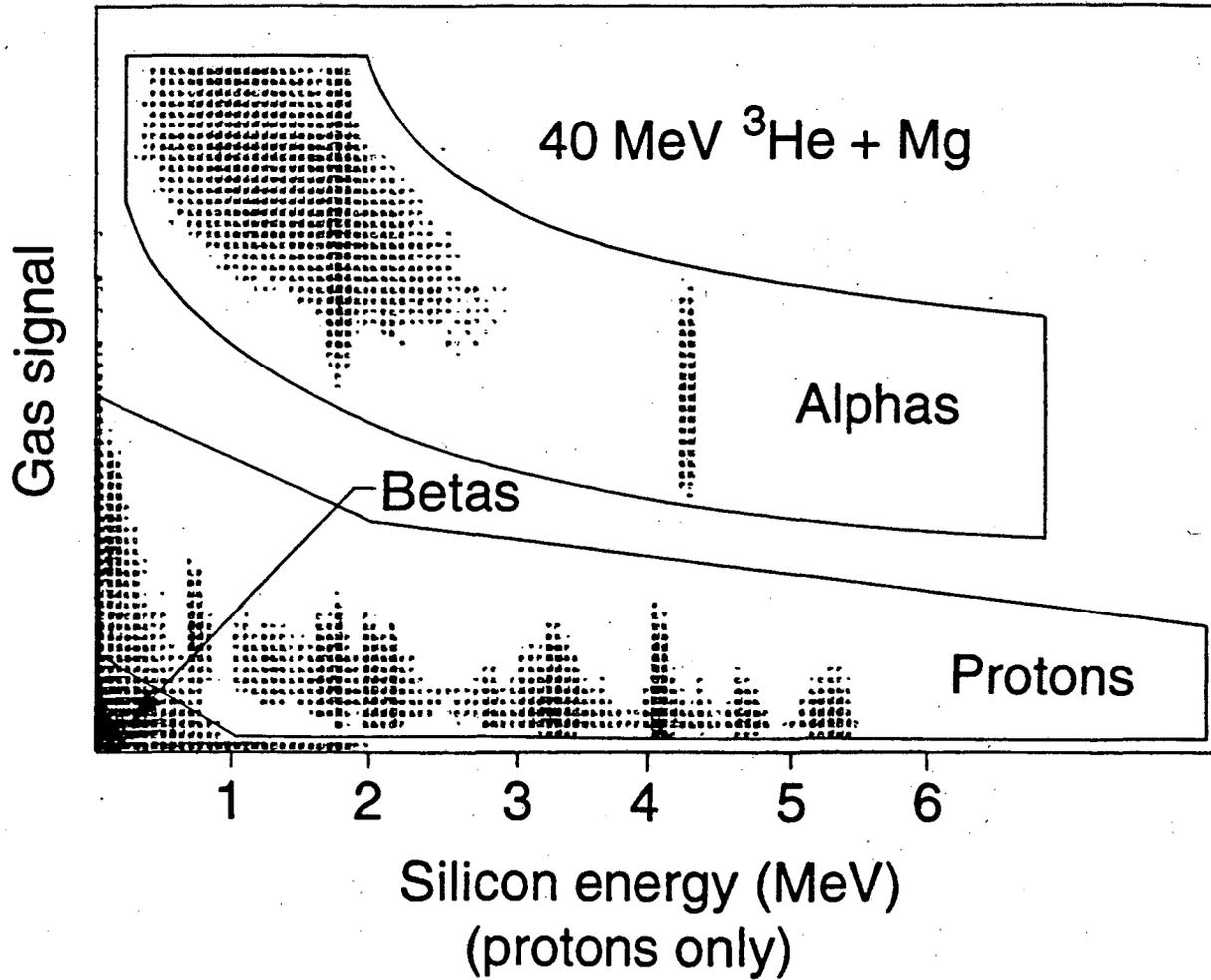
[e]Unquenched matrix elements.

FIGURE CAPTIONS

Fig. 1.   Experimental setup used to measure the beta-delayed proton spectrum of ^{25}Si.
Additional details may be found elsewhere [8].

Fig. 2.   Two-dimensional plot of the measured energy in the silicon E detector versus the
differential energy gas signal. The beta, proton and alpha groups are clearly shown
(alphas arise from ^{20}Na and ^{8}B beta-delayed alpha decay). In order to accurately
represent the normal color logarithmic scale in black and white, a small and uniform
background subtraction has been utilized.

Fig. 3.   Beta-delayed proton spectrum arising from ^{29}S decay. Peak energies were taken from
Reference [10].

Fig. 4.   Beta-delayed proton spectrum arising from the 40 MeV ^{3}He + ^{nat}Mg reaction. Peak
energies are listed in Table I.

Fig. 5.   Proposed partial decay scheme for ^{25}Si.

Fig. 6.   Plot of experimental and theoretical Gamow-Teller beta strength as a function of the
excitation energy in ^{25}Al. Additional details are in the text.

Helium
in

Target box

Target

HAVAR exit foils
(N$_2$ cooled)

Beam

HAVAR entrance foils
(N$_2$ cooled)

Slotted
collection
cylinder

Capillary

To
roots
blower

Detector
chamber

Detector
telescope

Si E

Gas ΔE

Rotating
catcher wheel

Detector Telescope Cross Section

1.40 cm

30 µg/cm^2 polypropylene
window

Wire grid at ground

0.25 cm   CF$_4$ at 10.3 torr

70 µg/cm^2 Ni foil at 520 V

CF$_4$ at 10.3 torr

Wire grid at ground

300 µm Si detector

XBL 927-5748

17

40 MeV ^{3}He + Mg

Alphas

Betas

Protons

Gas signal

Silicon energy (MeV)
(protons only)

XBL 927-5751

40 MeV ^{3}He + Si
26 mC

0.739
2.129
3.720
5.437

Counts

E_p (MeV)

XBL 927-5752

XBL 927-5753

J^π, T

5/2$^+$, 3/2   12.736

β^+ ~ ^{25}Si $t_{1/2} = 220.7$ ms
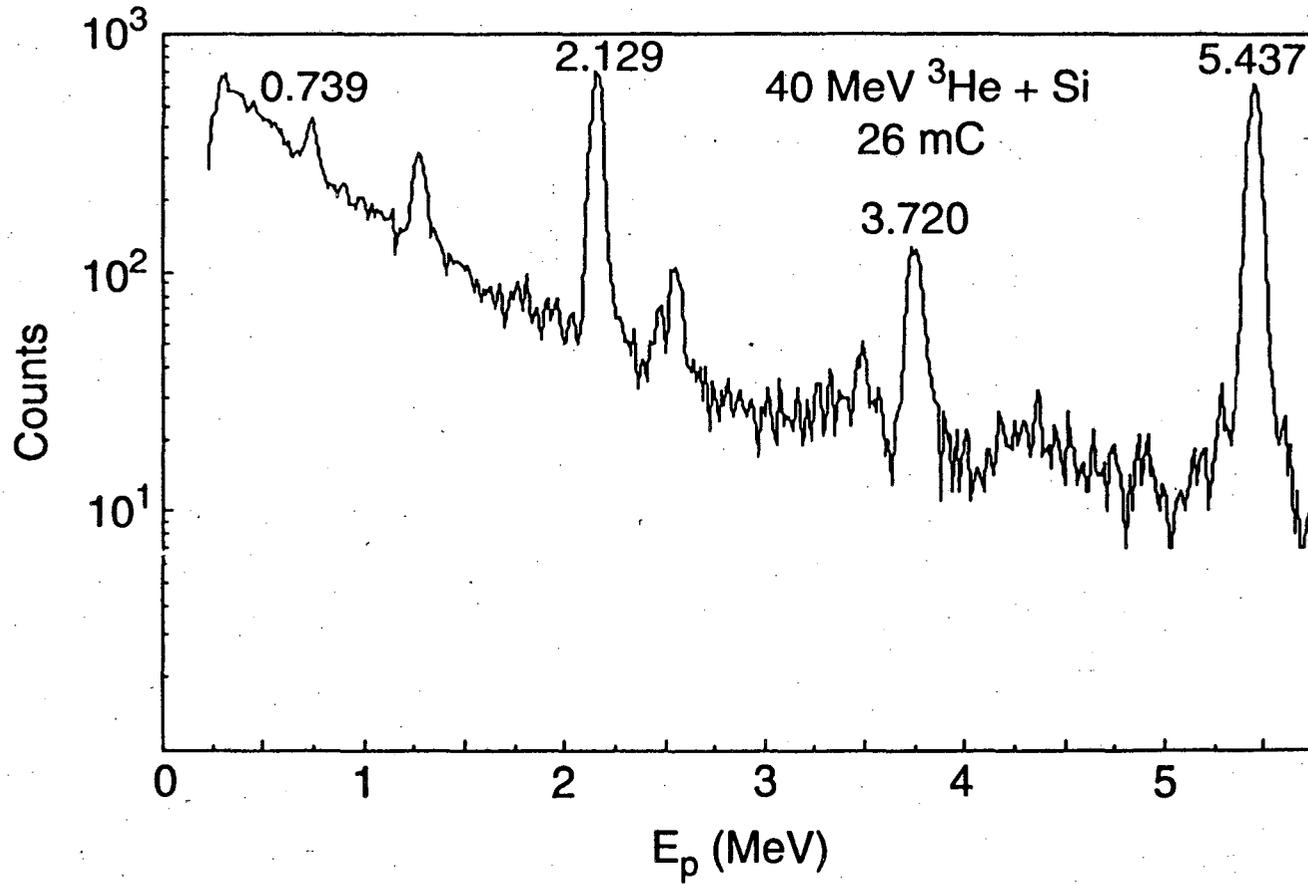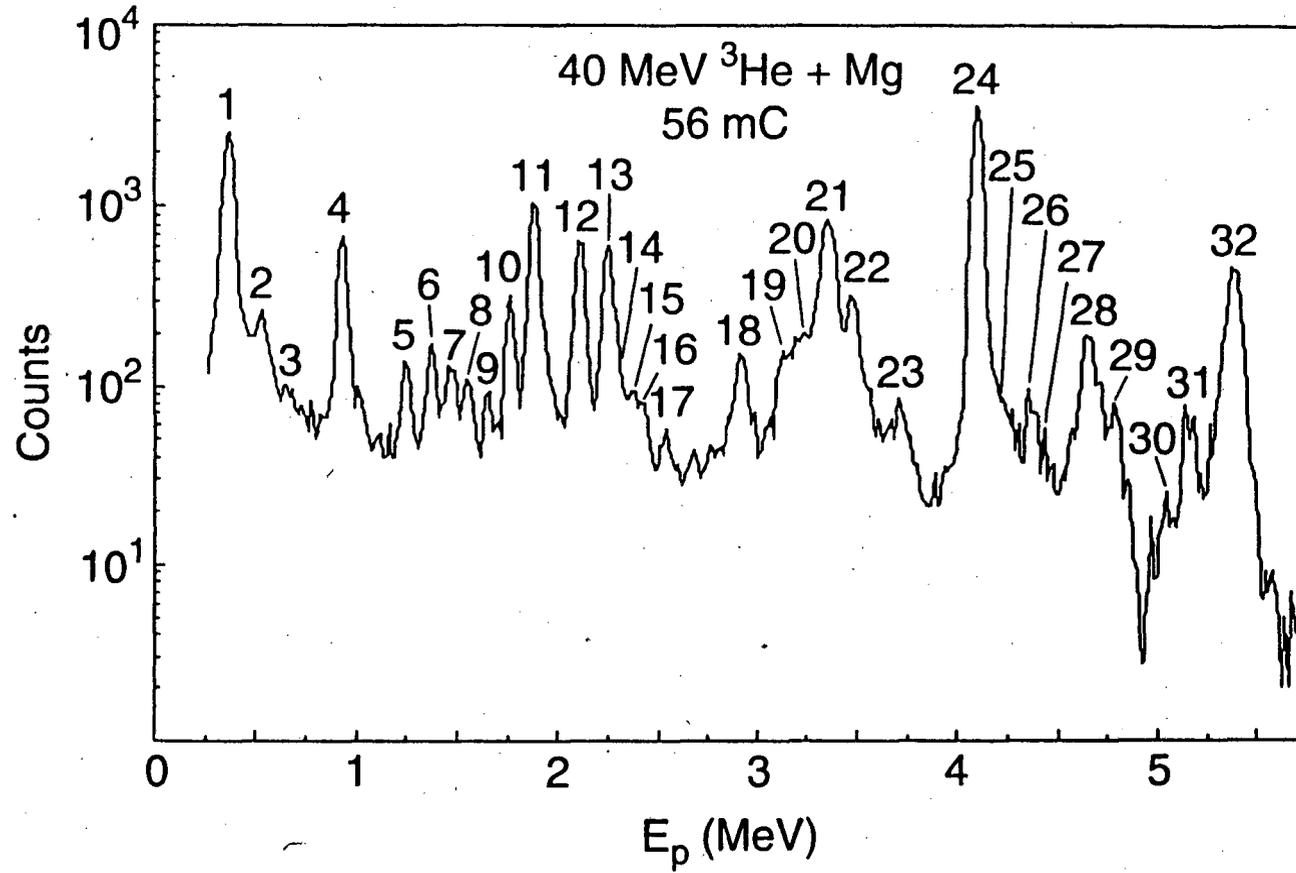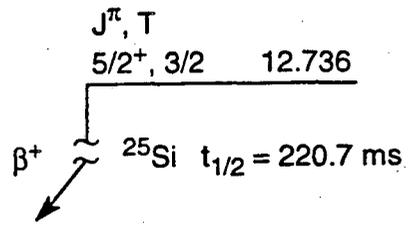
Energy	%β	log *ft*
8.193	0.89	4.26
7.936	0.33	4.83
7.901	**12.2**	**3.28** 5/2$^+$, 3/2
7.819	0.32	4.90
7.646	0.20	5.20
7.417	0.15	5.42
7.240	1.31	4.56
7.112	4.15	4.12
7.022	0.65	4.96
6.909	0.02	6.43
6.881	0.41	5.22
6.645	0.37	5.36
6.123	0.21	5.80
6.063	0.04	6.55
5.809	1.71	5.00
4.906	0.26	6.11
4.583	3.10	5.13
4.196	2.97	5.26
3.859	0.14	6.66
2.720	<0.4	>6.5
2.674	8.2	5.19
1.790	1.7	6.06
1.612	17.0	5.10
0.945	22.1	5.12
0.000	20.8	5.32

(3/2 - 7/2)$^+$

3$^+$ 7.507

2$^+$ 6.509

4$^+$ 6.384

(5/2, 7/2)$^+$

5/2$^+$

(3/2 - 7/2)$^+$

≥ 5/2$^+$

5/2$^+$

3/2$^+$

5/2$^+$

2$^+$ 3.639

3/2$^+$ 7/2$^+$

0$^+$ 2.271

^{24}Mg + p

5/2$^+$

7/2$^+$

3/2$^+$

5/2$^+$

^{25}Al

XBL 927-5749

21

GT strength

E_X (MeV)

0 1 2 3 4 5 6 7 8 9 10 11 12

0.6 0.4 0.2 0.0 0.2 0.4 0.6

☐ Experimental

■ Theoretical

XBL 927-5750

LAWRENCE BERKELEY LABORATORY
UNIVERSITY OF CALIFORNIA
TECHNICAL INFORMATION DEPARTMENT
BERKELEY, CALIFORNIA 94720